

# Optical and electrical properties of bismuth sulphide thin film prepared in PVA matrix by chemical drop method

A. HUSSAIN, A. BEGUM, A. RAHMAN\*

*Department of Physics, Gauhati University, Guwahati- 781014, India*

Nanocrystalline  $\text{Bi}_2\text{S}_3$  thin films were prepared by chemical drop method using polyvinyl Alcohol (PVA) as a matrix solution. Characterization of the films was carried out using X-ray diffraction (XRD), Scanning electron microscopy (SEM), optical absorption, composition analysis and electrical conductivity measurement. According to XRD spectra the deposited films were pure orthorhombic and sizes of the particles obtained were between 3-10nm. Surface morphology and particles sizes were also known from SEM images. Composition was also known from EDAX. The band gap obtained from the absorption spectra was found to change from 3.88 eV to 3.82 eV on changing the grain size from 3nm to 10nm. The absorption edge obtained from the spectra was found to shift towards the lower wavelength. The electrical conductivity at room temperature was found to be in the range  $10^{-6}\Omega^{-1}\text{m}^{-1}$ .

(Received March 12, 2010; accepted May 26, 2010)

*Keywords:* Semiconductors, Chemical synthesis, Electrical conductivity

## 1. Introduction

In the last few years, nanocrystalline semiconducting thin films occupied an important place in research work due to their future applications. The optical, electrical and magnetic properties of a material change on changing the grain size and thickness of the film [1]. So, it offers the possibility of materials enhancement device characteristics [2]. The particles with diameter in the range of 1-100 nm are in intermediate state between atomic and bulk species and their electronic structures are different from bulk materials [3,4]. The electronic bands split into discrete levels. The band structures of semiconducting materials are affected by the size of the nanocrystals and therefore properties are depending on the crystal size.

In this paper, we are focusing on chemical deposition, structural analysis, optical absorption and electrical conductivity of  $\text{Bi}_2\text{S}_3$  nanostructure in the temperature range 298K to 388K.  $\text{Bi}_2\text{S}_3$  which belongs to group V-VI compound semiconductor has band gap energy in the range (1.3-1.7eV) which lies in the visible region of the spectra [5-8]. The calculated work function of  $\text{Bi}_2\text{S}_3$  micro belts at the highly oriented {001} surfaces has been reported to be 4.93eV [9]. This indicates the potential application of this material for anode material and understanding the field emission characteristics and photochemical behaviours. It is very useful for solar energy conversion devices [10-12], photoelectronics devices, photo electrochemical devices, thermoelectric coolers, electric switching, solar selective coating etc [13,14].

$\text{Bi}_2\text{S}_3$  thin films have been reported to be prepared by different techniques such as ultrasonic method [15,16], microwave irradiation [17,18], hydrothermal synthesis [19-21], chemical deposition [22-27], solvothermal decomposition [28,29], thermal evaporation [24] and

reactive evaporation [30]. Here in our work, we are using chemical drop method which is convenient and has the advantage of economy and the ability to deposit large areas. With this method, size of the particles can be easily controlled by changing the concentration of different constituents of the solution. Nanoparticles of  $\text{Bi}_2\text{S}_3$  were prepared in a matrix of polyvinyl alcohol (PVA) and the same were studied for optical and electrical properties.

## 2. Experimental details

For the preparation of nanocrystalline  $\text{Bi}_2\text{S}_3$  thin films in polyvinyl alcohol (PVA),  $\text{Bi}(\text{NO}_3)_3$  and  $\text{Na}_2\text{S}$  were used as  $\text{Bi}^{+3}$  ion source and  $\text{S}^{-2}$  ion source respectively. First, the PVA matrix was prepared. For this, 5wt% of PVA solution was prepared in double distilled water and stirred with the help of a magnetic stirrer at a constant temperature 348K until a transparent solution was formed. To this solution, 0.03M (molarity) of  $\text{Bi}_2\text{S}_3$  was added in the ratio of 2:1 and the stirring was continued at the same temperature for 3 hrs and brought down at the room temperature (300K). To this solution, 0.03M of  $\text{Na}_2\text{S}$  was added drop by drop until the solution turned into dark brown. The resultant solution was kept in a dark chamber undisturbed for 12 hrs for stabilization. The stabilized solution was cast over the glass substrates drop by drop and dried at room temperature (300K). This way the films containing  $\text{Bi}_2\text{S}_3$  embedded in a PVA matrix were obtained. Three sets of films with different molarities (0.015M, 0.02M 0.03M) of  $\text{Bi}_2\text{S}_3$  were obtained using the above mention procedure. Films of higher molarity could not be prepared under the present condition because  $\text{Bi}(\text{NO}_3)_3$  of more than 0.05M could not be dissolved in PVA solution.

For the measurement of electrical conductivity of the films two types of electrode arrangement were made viz: gap type and sandwich type. In gap type structures conducting materials such as Al or In was vacuum deposited on the two sides of linear films keeping small gap in between. In sandwich type samples,  $\text{Bi}_2\text{S}_3$  films were deposited over vacuum deposited lower electrodes and over which top electrodes were vacuum deposited sandwiching the  $\text{Bi}_2\text{S}_3$  films in between the electrodes. The evaporation of electrodes was performed at a reduced pressure of  $10^{-5}$  Pa. Thus gap type as well as sandwich type samples such as Al- $\text{Bi}_2\text{S}_3$ -Al, In- $\text{Bi}_2\text{S}_3$ -In were fabricated. Electrical conductivity measurements were performed over a voltage range of 2V-7V using a stabilized power supply and a Keithley digital electrometer in the temperature range 298K to 388K and the same temperature was varied using a temperature controller. Temperatures of the samples were measured by means of a thermocouple.

### 3. Results and discussion

#### 3.1. XRD Studies

The X-ray diffractogram of the PVA-  $\text{Bi}_2\text{S}_3$  structures exhibit broadened diffraction profile. A broad peak has been observed around  $2\theta = 19.6^\circ$  as shown in fig 1. XRD spectrum of pure PVA shows similar peak around the same angle. This indicates that the XRD peak observed in PVA-  $\text{Bi}_2\text{S}_3$  complex is due to the PVA matrix. Since the  $\text{Bi}_2\text{S}_3$  particles are of nanosize and sparsely distributed in the PVA matrix, the diffracted beams from  $\text{Bi}_2\text{S}_3$  were not sufficiently intense to give any detectable peak.

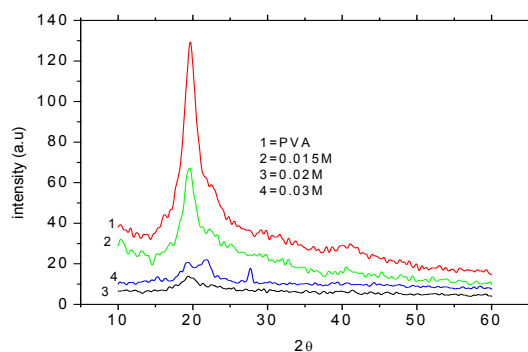


Fig. 1. X-Ray diffraction patterns of PVA- $\text{Bi}_2\text{S}_3$  thin films of different molarities.

Also some peaks if present were merged with the broad peak obtained from PVA. The crystallite size of the nanocrystalline films was estimated using Scherrer's formula [2]

$$d = \frac{4}{3} \frac{0.9\lambda}{\beta \cos \theta} \quad (1)$$

where  $\lambda$  is the wavelength of the X-ray used,  $\beta$  is the full width at half maximum of diffraction peak and  $\theta$  is the

Bragg's angle. The crystallite sizes were found to be 10.8nm, 4.7nm and 3.6nm for molarities 0.015M, 0.02M and 0.03M of  $\text{Bi}_2\text{S}_3$  respectively. It is observed that crystallite size decreases with increase in molarity.

#### 3.2. SEM analysis

Scanning Electron Microscopy is the convenient technique to study the surface morphology of thin films. Fig. 2 (a), (b) and (c) shows the surface morphology of a typical PVA-  $\text{Bi}_2\text{S}_3$  complex deposited at room temperature. It is observed that grains of  $\text{Bi}_2\text{S}_3$  are not uniformly distributed throughout the PVA matrix. But the film is smooth without any void or crack. From this image, it is seen that the grain sizes of the films are not uniform. Therefore, average grain sizes were estimated of different grains within the film and found to be in the range of 41.95-117 nm. It is quite clear from the results that the average grain size estimated by SEM is larger than the average grain size measured by XRD.

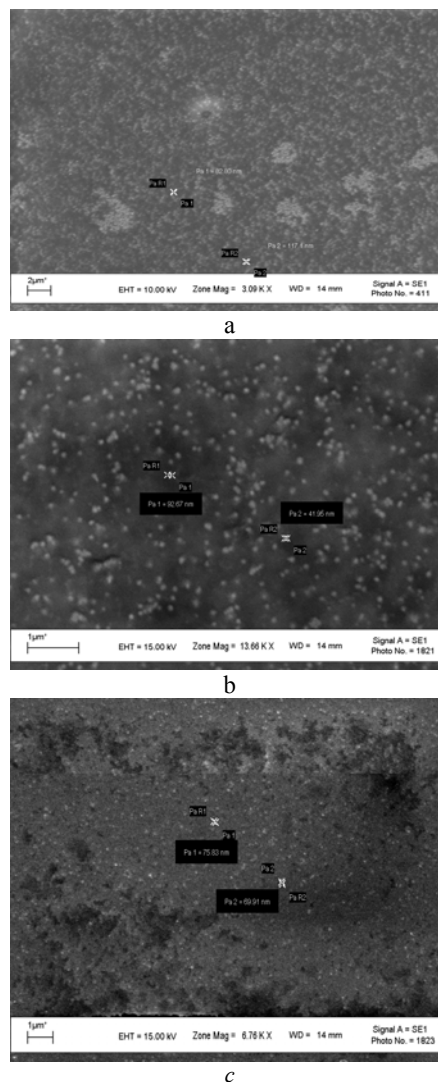


Fig. 2 (a) SEM photograph of 0.015M, (b) SEM photograph of 0.02M, (c) SEM photograph of 0.03M.

### 3.3. EDAX study

Fig. 3 gives the quantitative analysis by EDAX of  $\text{Bi}_2\text{S}_3$  thin films deposited on a glass substrate at room temperature. The elemental analysis was carried out only for Bi and S, the average atomic percentage of Bi:S was 77:22, (i.e. 3 : 1 ratio), showing that the sample was S deficient.

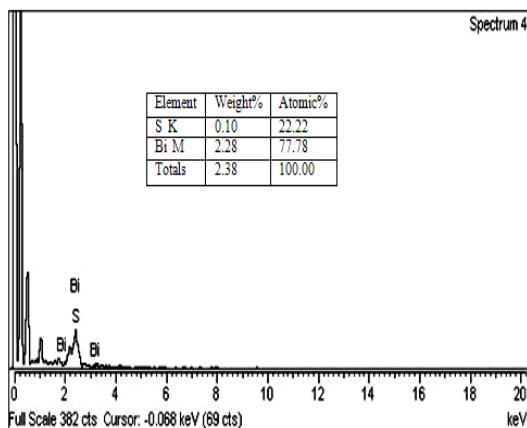


Fig. 3. EDAX spectrum of 0.015 M

### 3.4. Absorption studies

Fig. 4 (a) shows the absorption spectra of three different  $\text{Bi}_2\text{S}_3$  thin films prepared in PVA matrix. From the spectra the absorption edges of the samples are found to occur at 330nm, 335nm and 340nm for 0.03M, 0.02M and 0.015M samples respectively. The absorption edge shows a clear shift towards lower wavelength. This blue shift of the absorption edge indicates decrease of the crystallites sizes of the particles causing a change in the optical band gap energy. The nature of the transition is determined by the relation

$$\alpha = a \frac{(h\nu - E_g)^n}{h\nu} \quad (2)$$

Where 'a' is constant and  $E_g$  is the separation between the conduction band and valence band. If the plot of  $(\alpha h\nu)^{1/2}$  vs  $h\nu$  is linear, then the transition is known as an indirect band edge transition and if the plot of  $(\alpha h\nu)^2$  vs  $h\nu$  is linear, then such a transition is known as direct band edge transition. The linear nature of the plot indicates the existence of the direct transition. The extrapolation of the linear portion of such a plot to  $\alpha = 0$  yields the band gap as shown in figure 4 (b). The absorption co-efficient ' $\alpha$ ' was measured from relation

$$\alpha = 2.303 \left( \frac{A}{t} \right) \quad (3)$$

Where 'A' is the absorbance and 't' is the thickness of the film. The band gap obtained from the fig.3.4(b) were 3.82eV, 3.85eV and 3.88eV for molarity 0.015M, 0.02M and 0.03M respectively.

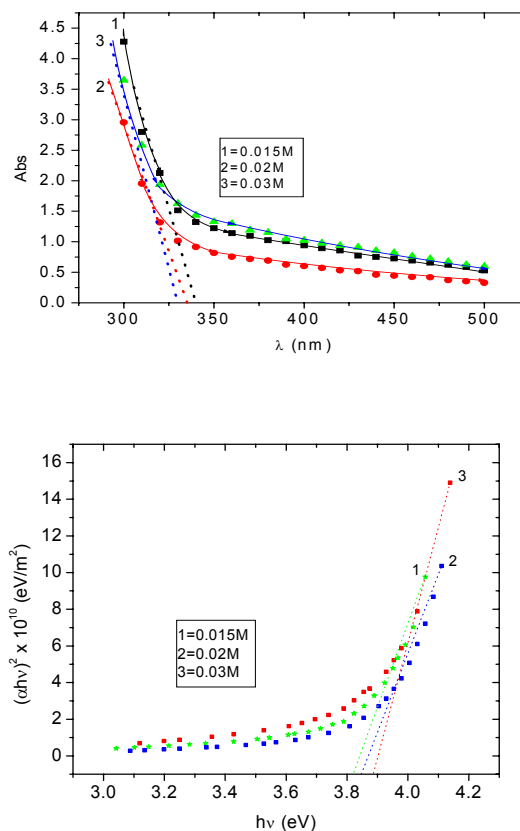


Fig. 4.(a) UV-absorption spectra of  $\text{Bi}_2\text{S}_3$  nanocrystalline films for different molarities, (b) Energy band determination of  $\text{Bi}_2\text{S}_3$  films for different molarities from the  $h\nu$  vs  $(\alpha h\nu)^2$  graph.

### 3.5. Electrical conductivity

The electrical conductivity measured on gap type sample using Al and In as electrode materials has been shown in fig.5(a) and 5(b) respectively and that of sandwich type sample using In as electrode materials has been shown in fig.5(c) for the temperature ranging from 298K to 388K. The conductivity has been observed to increase in all the sample as the temperature raised from 248K attaining a maximum around 323K, after which the conductivity was found to decrease and reached a minimum around 333K beyond which the conductivity showed a sharp increase again. This variation of conductivity has been thought to be due to phase transition with change in temperature. The temperature variation of conductivity of PVA was also studied with same electrode and has been observed to exhibit same pattern of variation of conductivity as stated above. The value of conductivity of PVA was of the order of  $10^{-7} \Omega^{-1} \text{m}^{-1}$  while that of the  $\text{Bi}_2\text{S}_3$ -PVA complex was of the order of  $10^6 \Omega^{-1} \text{m}^{-1}$ . Thus, it may be inferred that the conductivity of  $\text{Bi}_2\text{S}_3$  thin films grown in PVA matrix is largely influenced by the conductivity of PVA. More than one straight line are

obtained in the  $\log(\sigma)$  vs  $1/T$  curves (region I and region II) with different activation energies, indicating different conduction processes such as electronic and ionic conduction [31-32]. M. A. Ahmed and M. S. Abo-Elil [33] reported conductive processes to be electronic in co-operation with ionic in Vanadate doped PVA. They have also observed a phase transition regions from 360K to 380K. Abdel-Malik, R. M. Abdel-Latif, A. sawaby and S. M. Ahmed [34] explained current transport mechanisms in pure and doped PVA films in terms of both schottky and Pool-Frenkel effects. The Thermal activation energies were calculated using the relation

$$\sigma = \sigma_0 e^{-\frac{E_a}{2kT}} \quad (4)$$

where  $E_a$  is the activation energy,  $\sigma_0$  is a constant,  $k$  is the Boltzman's constant and  $T$  is the absolute temperature. Activation energies of PVA and different PVA-Bi<sub>2</sub>S<sub>3</sub> films were calculated in the regions I and II. Average activation energies obtained from the slopes in the region I and II of pure PVA were 1.166eV and 0.657eV respectively and the same for nanostructured Bi<sub>2</sub>S<sub>3</sub> grown in PVA are 1.36eV and 0.62eV.

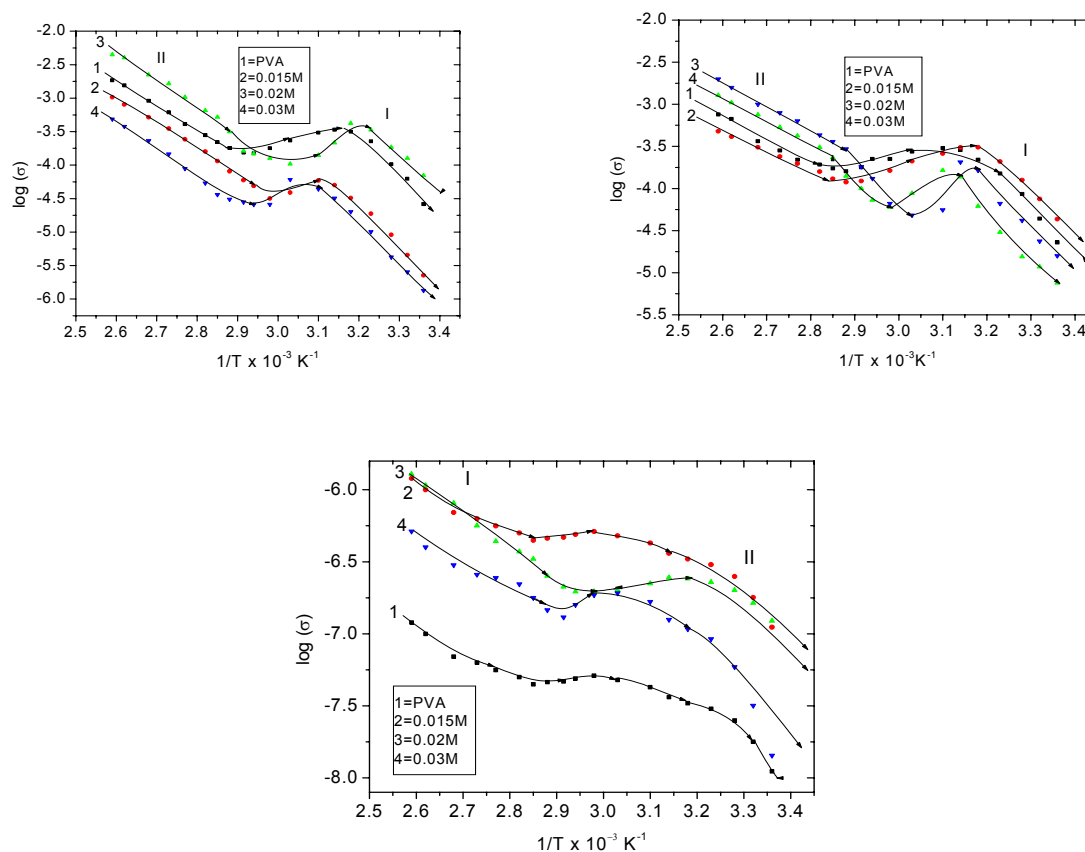


Fig. 5. Variation  $\log(\sigma)$  vs reciprocal of temperatures for different molarities of PVA-Bi<sub>2</sub>S<sub>3</sub> thin films and PVA using Al and In electrode. (a) Al-PVA-Bi<sub>2</sub>S<sub>3</sub>-Al gap type, (b) In-PVA-Bi<sub>2</sub>S<sub>3</sub>-In gap type, (c) In-PVA-Bi<sub>2</sub>S<sub>3</sub>-In sandwich type.

### 3.6. Conclusions

Thin films of Bi<sub>2</sub>S<sub>3</sub> prepared by chemical drop method in PVA matrix were found to be nanocrystalline. The crystallite sizes measured by XRD studies were found to be within 3.6-10.8nm and from SEM within 41.95-117nm for the same set of samples. The crystallite size has been found to decrease with increase of molarity. The band gap energy has been found to increase with decrease in crystallite size showing a blue shift in the absorption spectra. The electrical conductivity of pure PVA and PVA-Bi<sub>2</sub>S<sub>3</sub> were found in the range of  $10^{-7}\Omega^{-1}\text{m}^{-1}$  and

$10^{-6}\Omega^{-1}\text{m}^{-1}$  respectively. The PVA matrix has exhibited phase transition around 320K to 350K. Electronic as well as ionic conduction processes are thought to be operative.

### Acknowledgement

We express our gratefulness to the Department of instrumentation & USIC, Gauhati university, Guwahati and IIT, Guwahati for providing us the XRD and SEM facilities.

## References

- [1] A. Tanaka, S. Onari, T. Arai, *Phys Rev*, **B47**, 1237 (1993)
- [2] Biljana Pejova, Ivan Grozdanov, *Mat. Chem. and Phys*, **99**, 39 (2006).
- [3] K Akamatsu, S. Deki, *Nanostructure Mater* **8**, 1121 (1998)
- [4] R. Kubo, *J. Phys. Soc. Jpn*, **17**, 975 (1962).
- [5] C.D. Lokhande, *Mater chem. physics* **27** (1991).
- [6] D. Jason Riley, Jonathan P. Waggett, K.G. Upul Wijayantha, *J. mater chem*, **14**, 704 (2004).
- [7] M. Gratzel, *Nature*, **414**, 338 (2001).
- [8] D. Cummins, G. Boschloo, M. Ryan, D. Corr, S.N. Rao, D. Fitzmaurice. *J.Physics. Chem, B* **104**, 11449 (2000)
- [9] Yu Zhao, Xi Zhu, Yanyan Huang, Sunki Wang, Jinlong, Yi Xie. *J.Phys. Chem. C*, **111**(33), 12141 (2007).
- [10] A.B. Novoselova(Ed). *Physical and chemical properties of semiconductor handbook*, Nauka, Moscow, 1978, P. 97.
- [11] N. Parhi, B.B. Nayak, B.S. Acharya. *Thin solid films*, **254**, 47 (1995).
- [12] I.M. Chapnik, *Phys. Stat. Sol.(B)* **137**, K95 (1986).
- [13] S. R. Gadakh, C.H. Bhosale, *Mater. Res. Bull.* **35**, 1097 (2000).
- [14] V. V. Killerdar, C. D. Lokhande, C. H. Bhosale. *Thin solids films*, **289**, 14 (1996).
- [15] S. Y. Wang, Y.W. Du. *J.Crystal growth* **236**, 627 (2002).
- [16] H. Wang, J.J. Zhu, J.M. Zhu and H.Y. Chen, *J. Physics. Chem, B*, **106**, 3848 (2002).
- [17] X. H. Liao, J.J. Zhu, and H.Y. Chen, *Mater Sci. Eng, B*, **85**, 86 (2001).
- [18] X. H. Liao, H. Wang, J. J. Zhu, H. Y. Chen, *Mater. Res. Bull*, **233**, 799 (2001).
- [19] M.W. Shao, M.S. Mo, Y. Cui, G. Chem and Y.T. Qian, *J.Crystalgrowth* **233**, 799 (2001).
- [20] M.X. Zhang, Z.H. Yang, X.M. Huang, S.Y. Zhang, W.C. Yu, Y.B. Jia, G.I. Zhou, L. Chem, *Solid state communication*, **119**, 143 (2001).
- [21] S. H. Yu, J. Yang, Y.S. Yu, Z.H. Han, Y. Xie, Y.T. Qian, *Mater Res. Bull.* **33**, 1611 (1998).
- [22] R. S. Mane, C.D. Lokhande, B.R. Sankapal, *Mater. Res. Bull*, **35**, 587 (2000).
- [23] R. S. Mane and C.D. Lokhande, *Mater Chem. Phys*, **65**, 1 (2000).
- [24] M. E. Rincon, M. Sanchez, P.J. George, A. Sanchez P.K. Nair, *J. Solid State chem*, **136**, 167 (1998).
- [25] P. K. Nair, M.T.S. Nair, V.M. Garcia, O. L. Arenas, Y. Pena, A. Castillo, I.T. Ayala, O. Gomezdza, A. Sanchez, J. Cumpos, H.U.R. Saurez, M.E. Rincon, *Sol. Energy. Mater. sol. cells*, **52**, 313 (1998).
- [26] L. Huang, P.K. Nair, M.T.S. Nair, R.A. Gingaro, E.A. Meyers, *Thin solid Films*, **268**, 49 (1995).
- [27] M. T. S. Nair, P.K. Nair, *Semiconductor Science Technology*, **5**, 1225 (1990).
- [28] S. H. Yu, L. Shu, J.A. Yang, Z.H. Han, Y.T. Qian, Y.H. Yang, *J.Mater Res*, **14**, 4157 (1999).
- [29] S. H. Yu, L. Shu, L. Yang, Y. Xie, Y.T. Qian, C.S. Wang, *Matter.Lett*, **35**, 116 (1998).
- [30] J. Lukose and B. Pradeep, *Solid State communication*, **14**, 4157 (1991).
- [31] A. K. Jonscher, *ibid.* **1**, 1213 (1967).
- [32] K. C. Kao, W. Hwang, *Electrical transport in solids*, (Pergamon Press, Oxford, 1981).
- [33] M. A. Ahmed, M. S. Abo-Ellil, *Journal of materials science: materials in electronics*, **9**, 391 (1998).
- [34] T. G. Abdel-Malik, R. M. Abdel-Latif, A. Sawaby, S. M. Ahmed, *Journal of applied sciences research*, **4**(3), 331 (2008).

\*Corresponding author: amir\_795130@yahoo.co.in